Supporting Information

Integrating High Mechanical Strength, Excellent Healing Ability, and Antibacterial Ability into Supramolecular Poly(Urethane-Urea) Elastomers by Tailoring the Intermolecular Supramolecular Interactions

*Yang Xu[a], Zhirong Xin[a], Shunjie Yan[b], Changjiang Yu[b], Jianyu Liu[a], Yanlong Yin[a], Peng Xu[b], Rongtao Zhou[b], Zhenlong Sun[b], Yusheng Qin[*a], and Chunyang Bao[*a]*

[a]College of Chemistry & Chemical Engineering, Yantai University, Yantai 264005, China.

[b]National Engineering Research Center of Implantable & Interventional Medical Devices and Materials, WEGO Holding Company Limited, Weihai 264210, China

Corresponding authors: baochunyang_chem@163.com; ysqin@ytu.edu.cn

1. Experimental Section.

1.1 Materials. Poly (tetramethylene ether glycol) (PTMEG, M_n 1000 g mol^{-1}), Isophorone diisocyanate (mixture of isomers) (IPDI), 4,4'-Methylenebis (cyclohexylamine) (mixture of isomers) (HMDA), Ditin butyl dilaurate (DBTDL) were purchased from Shanghai Aladdin Biochemical Technology Co., Ltd. *N,N*-Dimethyl acetamide (DMAc, 99.8% Extra Dry) were purchased from Energy Chemical Technology (Shanghai) Co., Ltd. Curcumin was purchased from Shanghai Macklin Biochemical Co., Ltd. Tetrahydrofuran (THF) was purchased form Tianjin Fuyu Fine Chemical Co., Ltd.

1.2 Characterization. ^{1}H NMR spectra were recorded on a 400 MHz Bruker instrument using $CDCl_3$ as solvent at room temperature. The molecular weight and polydispersity (PDI) of the polymer was determined by gel permeation chromatography (GPC) on a Waters 2414 binary system with a refractive index detector, calibrated with polystyrene standards. The column temperature was maintained at 40 °C during the test using THF as the eluent at a flow rate of 1.0 mL/min. The FT-IR spectra of $SPUU_x$ elastomers and $SPUU_x$-Cur_y composites were performed on a Thermo Scientific Nicolet iS20 spectrometer in ATR mode between 600 cm^{-1} and 4000 cm^{-1} at room temperature. The thermal stability analysis was determined on a Netzsch TG 209 F3 Thermogravimetric analyzer under the nitrogen atmosphere. Each sample (~10 mg) was heated from 25 to 800 °C with a rate of 10 °C/min. Dynamic thermomechanical analysis were carried out on a Dynamic Mechanical Analyzer (DMA) TA Instrument Q800 using tension film mode with a frequency of 1 Hz and strain amplitude of 1%. The temperature ramp ranged from -100 to 130 °C with a heating rate of 5 °C/min. Stress-relaxation experiment was carried out on the DMA Q800 analyzer. The regular sample (30 mm × 5 mm × 1 mm) was first straightened by a force of 0.001 N, and then heated to the setting temperature. The target temperature was kept for 5 min to achieve thermal equilibrium. Then, the specimen was stretched at a constant strain of 50% to maintain deformation and the stress change was collected over time. All the stress-strain curves were performed on a UTM4103 Tension Instrument (Shenzhen SUNS Technology Co.

LDT, China) with a stretching speed of 50 mm/min at a temperature of 22 °C and relative humidity of ~20%. Young's modulus values were determined by the slope of the stress-strain curve in the initial linear region within the strain of 5%. The toughness is defined as the area surrounded by the stress-strain curves. The fracture energy was measured with Single notch drawing method, in which a single notch specimen was used for the determination of tear resistance. The fracture energy (G_c) was calculated by the following equation：

$$G_c = \frac{6wc}{\sqrt{\lambda_c}}$$

where c represents the length of the slit (1 mm), w represents the strain energy calculated by integration of the stress-strain curve of the unnotched specimen until ε_c, $\lambda_c = \varepsilon_c + 1$.

1.3 Antibacterial experiment. Before the antibacterial experiment, all the instruments and equipment were aseptically treated. $SPUU_x$-Cur_y and PE control films with the size of 1.5 × 1.5 cm^2 were placed in a 6-well plate and *S. aureus* suspension (25 μL) was added at the center region of the films. PE film was used to cover the *S. aureus* suspension subsequently. After cultivated at 37 °C for 6 h, the samples were immersed in 1 mL of phosphate-buffered saline (PBS) buffer and the adherent bacteria was released into PBS solution via ultrasound. The bacterial stock solution (80 μL) was dropped onto the medium, evenly coated, and cultured in an incubator at 37 °C for 24 h for colony counting.

2.Supplementary Figures and Table

Table S1. Specific molar ratios of $SPUU_x$ elastomers.

	PTMEG-1000 (mmol)	IPDI (mmol)	IPDA (mmol)
$SPUU_{1.7}$	6	10.2	4.71
$SPUU_{1.8}$	6	10.8	5.34
$SPUU_{2.2}$	6	13.2	7.86

Table S2. Molecular weight and the polydispersity index of $SPUU_x$ elastomers.

	M_n	M_w	PDI
$SPUU_{1.7}$	43000	61000	1.42
$SPUU_{1.8}$	38000	58000	1.52
$SPUU_{2.2}$	21000	32000	1.50

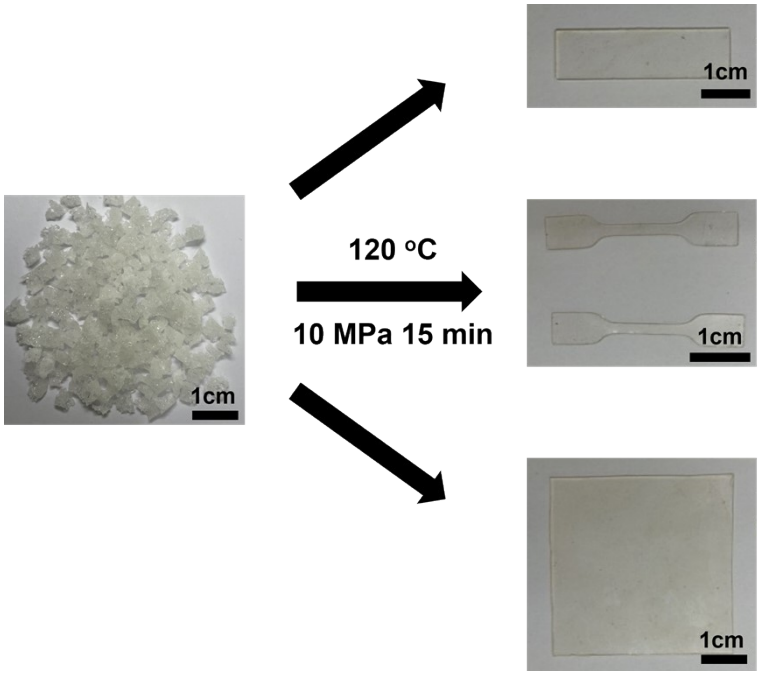

Figure S1. Images of the $SPUU_{2.2}$ elastomers that can be hot-pressed into various shapes under 120 °C and 10 MPa for 15 min.

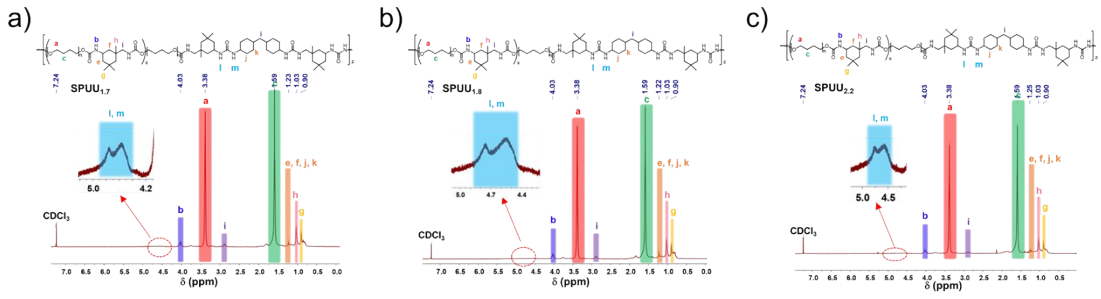

Figure S2. ^1H NMR spectra (400 MHz, $CDCl_3$) of $SPUU_x$ elastomers.

Table S3. Summary of the mechanical properties of the different SPUU$_x$.

Samples	Breaking strength (MPa)	Elongation at break (%)	Toughness (MJ m^{-3})	Young's modulus (MPa)
SPUU$_{1.7}$	30.5 ± 1.4	1554 ± 50	131.9 ± 2	1.6 ± 0.3
SPUU$_{1.8}$	43.2 ± 1.5	1151 ± 50	154 ± 26	3.3 ± 0.1
SPUU$_{2.2}$	42.3 ± 2.4	895 ± 52	139 ± 19	17.9± 0.3

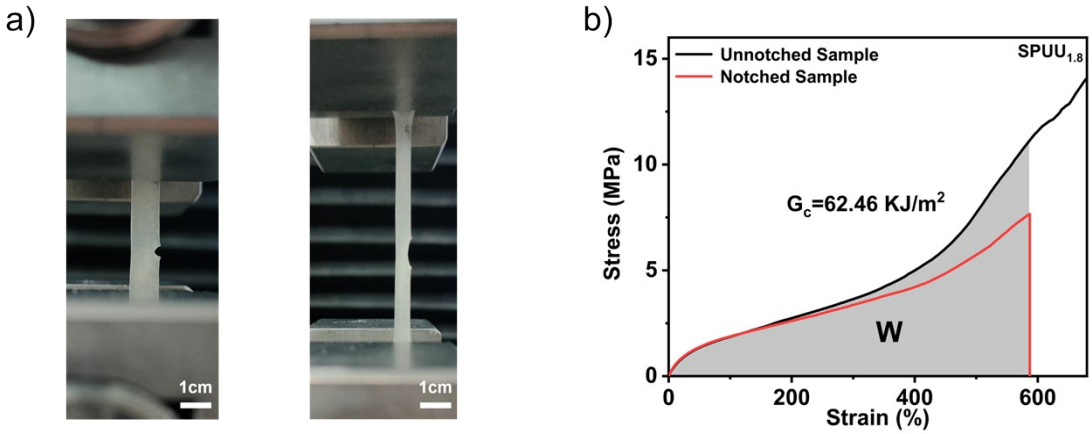

Figure S3. a) Images of the stretching process of the SPUU$_{1.8}$ samples with 1 mm notched. b) Typical stress-strain curves of non-notched and notched SPUU$_{1.8}$ samples.

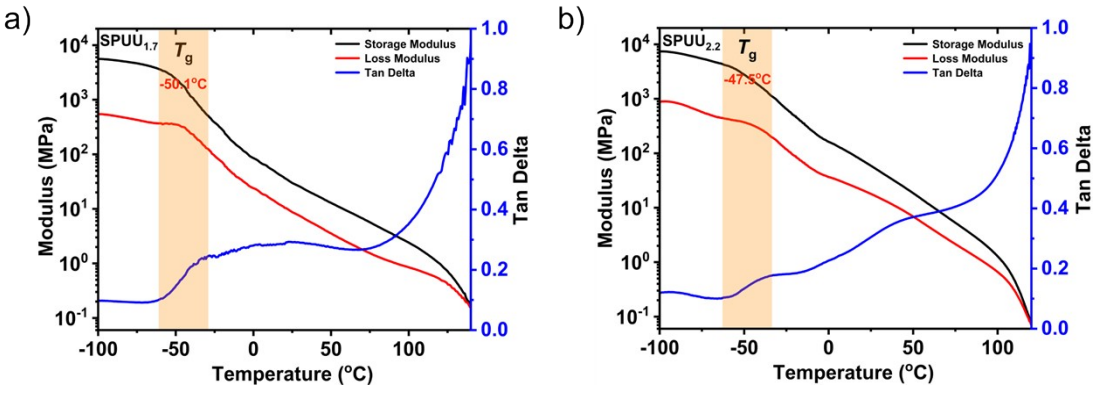

Figure S4. DMA curves of a) SPUU$_{1.7}$ and b) SPUU$_{2.2}$ elastomers.

Table S4. Thermal data of $SPUU_{1.7}$, $SPUU_{1.8}$, $SPUU_{2.2}$, and $SPUU_{1.8}$-Cur_y.

Samples	Weight loss temperature / °C		T_{HRI}* / °C
	5 wt.%	30 wt.%	
$SPUU_{1.7}$	297.2	349.2	160.9
$SPUU_{1.8}$	302.2	351.8	162.6
$SPUU_{2.2}$	301.5	347.1	161.1
$SPUU_{1.8}$-$Cur_{0.5\%}$	305.7	354.8	164.2
$SPUU_{1.8}$-$Cur_{1\%}$	304.3	354.0	163.7
$SPUU_{1.8}$-$Cur_{3\%}$	306.1	358.7	165.4
$SPUU_{1.8}$-$Cur_{5\%}$	303.3	359.2	165.1
$SPUU_{1.8}$-$Cur_{10\%}$	301.8	363.1	165.9
$SPUU_{1.8}$-$Cur_{15\%}$	298.2	367.1	166.4

*T_{HRI}=0.49×[T_5+0.6×(T_{30}-T_5)]. T_5 and T_{30} correspond to the decomposition temperature of 5 wt.% and 30 wt.% weight loss, respectively.

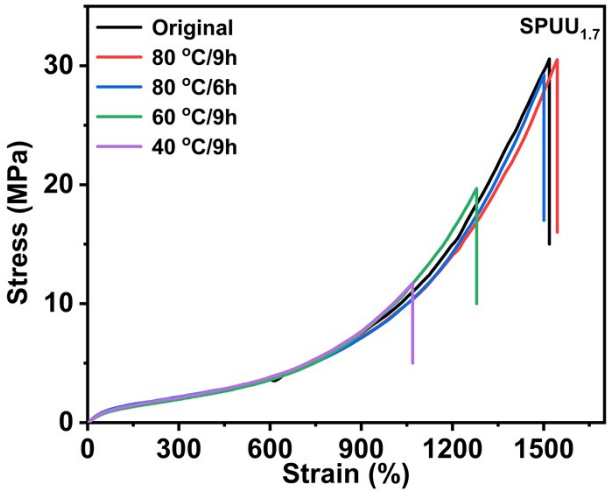

Figure S5. Stress-strain curves of $SPUU_{1.7}$ samples healed at different temperatures for 6 h and 9 h.

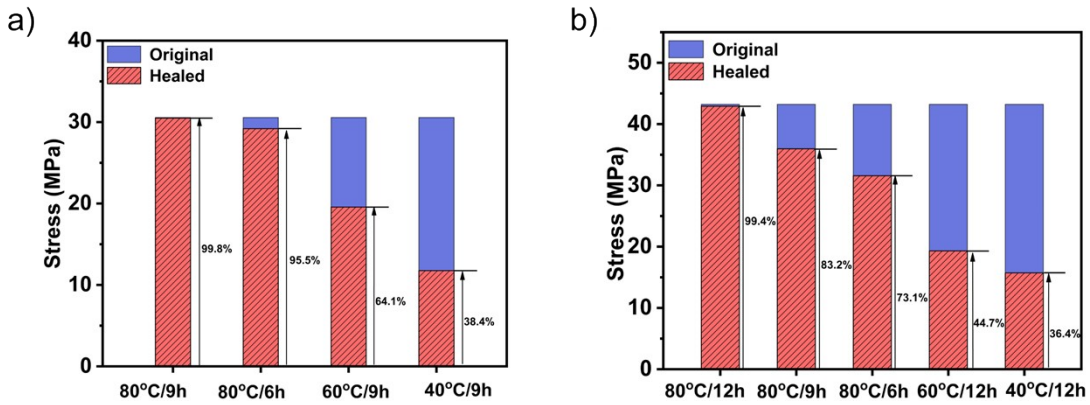

Figure S6. Healing efficiency of $SPUU_{1.7}$ and $SPUU_{1.8}$ elastomers.

.

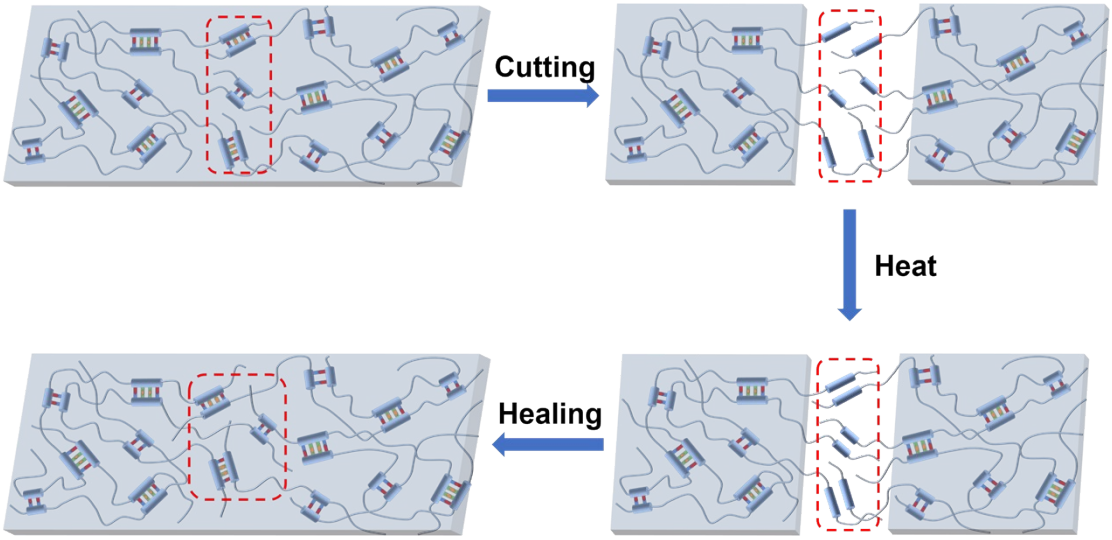

Figure S7. Healing mechanism of $SPUU_x$ elastomers.

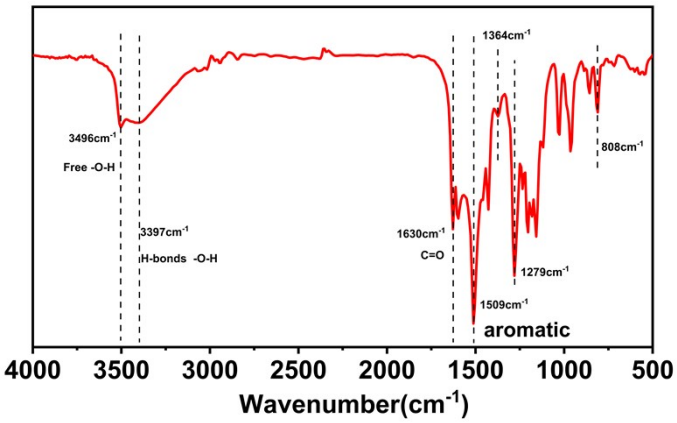

Figure S8. FT-IR spectrum of the curcumin from the wavelength of 500 cm^{-1} to 4000 cm^{-1}.

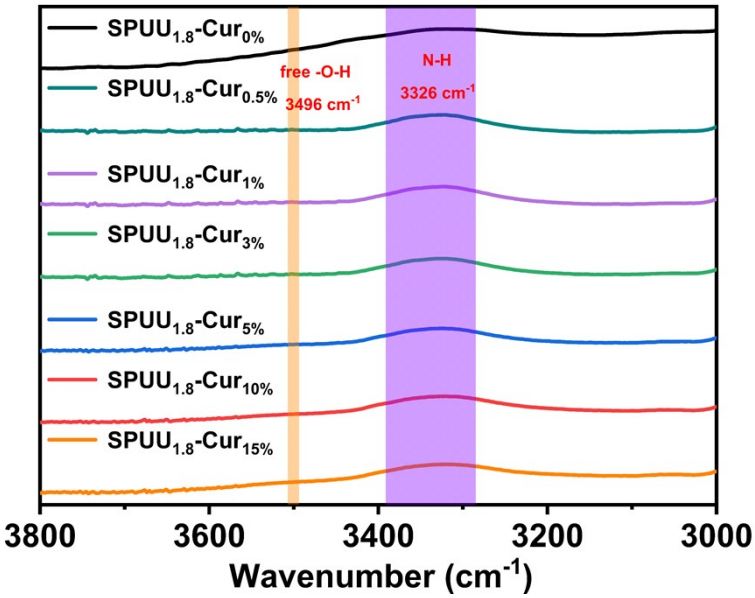

Figure S9. ATR-FTIR spectra of the $SPUU_{1.8}$-Cur_y composites from the wavelength of 3000 cm^{-1} to 3800 cm^{-1}.

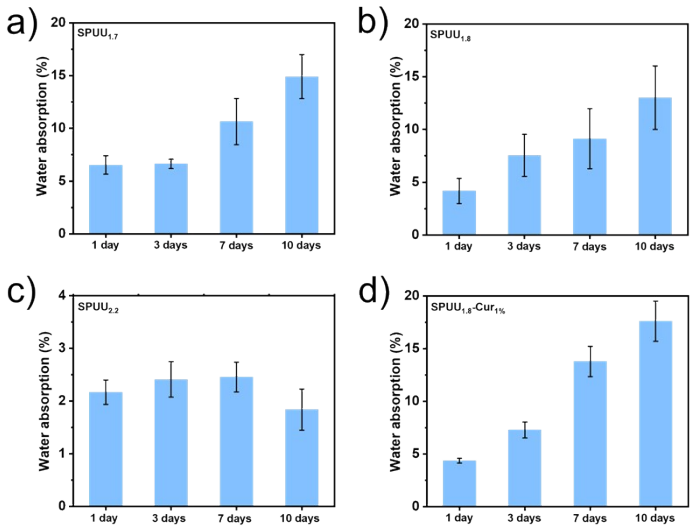

Figure S10. Water absorption of a) $SPUU_{1.7}$, b) $SPUU_{1.8}$, and c) $SPUU_{2.2}$, and $SPUU_{1.8}$-$Cur_{1\%}$ elastomers after immeresed in water for 1 day, 3 days, 7 days, and 10 days.

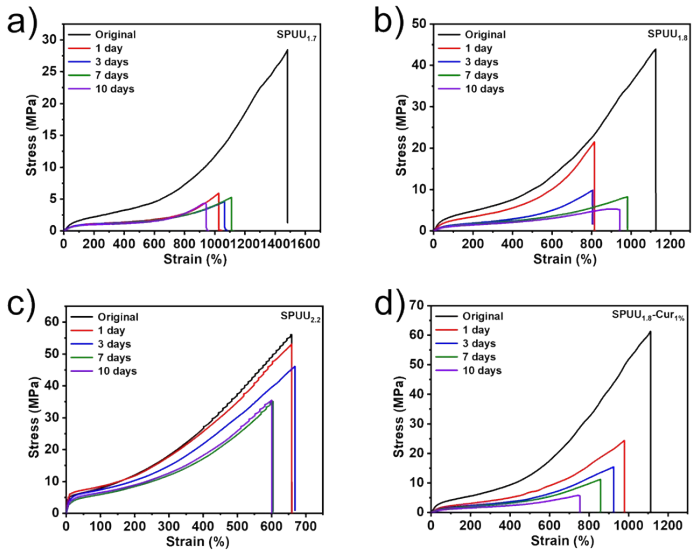

Figure S11. Stress-strain curves of a) $SPUU_{1.7}$, b) $SPUU_{1.8}$, and c) $SPUU_{2.2}$, and $SPUU_{1.8}$-$Cur_{1\%}$ elastomers after immeresed in water for 1 day, 3 days, 7 days, and 10 days.

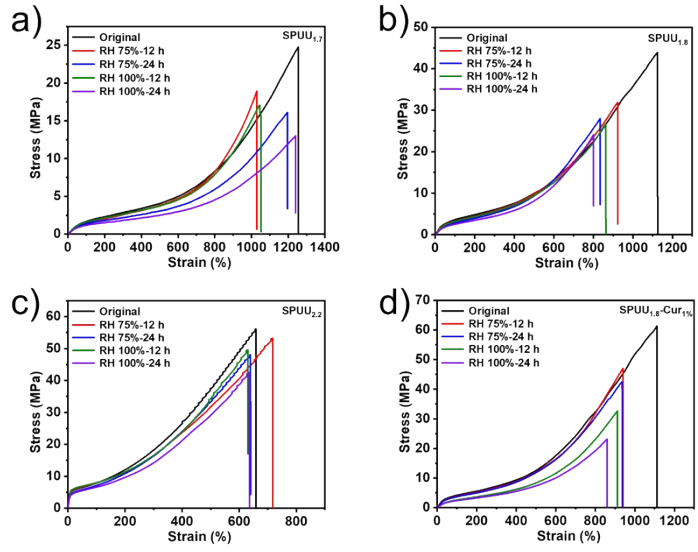

Figure S12. Stress-strain curves of a) $SPUU_{1.7}$, b) $SPUU_{1.8}$, and c) $SPUU_{2.2}$, and $SPUU_{1.8}$-$Cur_{1\%}$ elastomers after treating at 75% RH and 100% RH for 12 h and 24 h respectively.

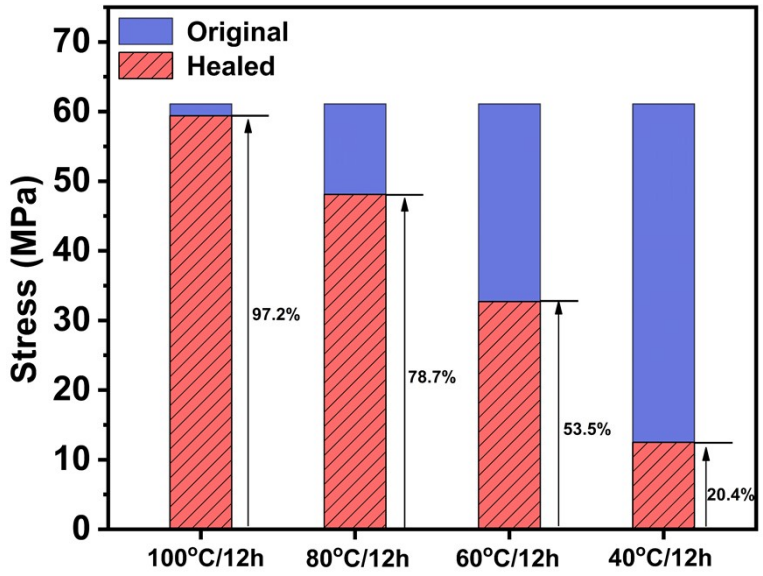

Figure S13. Comparation of the healing efficiency of $SPUU_{1.8}$ elastomers and $SPUU_{1.8}$-$Cur_{1\%}$ composites.

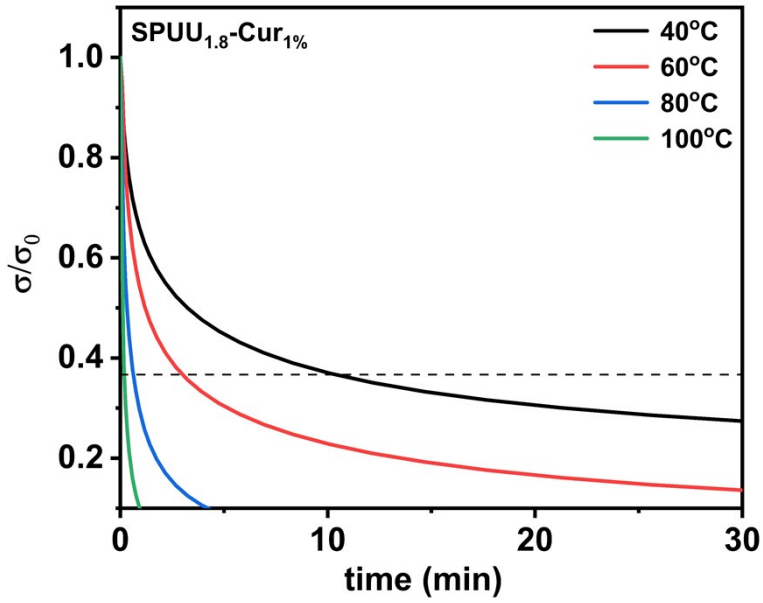

Figure S14. Stress-relaxation behavior of $SPUU_{1.8}$-$Cur_{1\%}$ composites at 40 °C, 60 °C, 80 °C, and 100 °C.

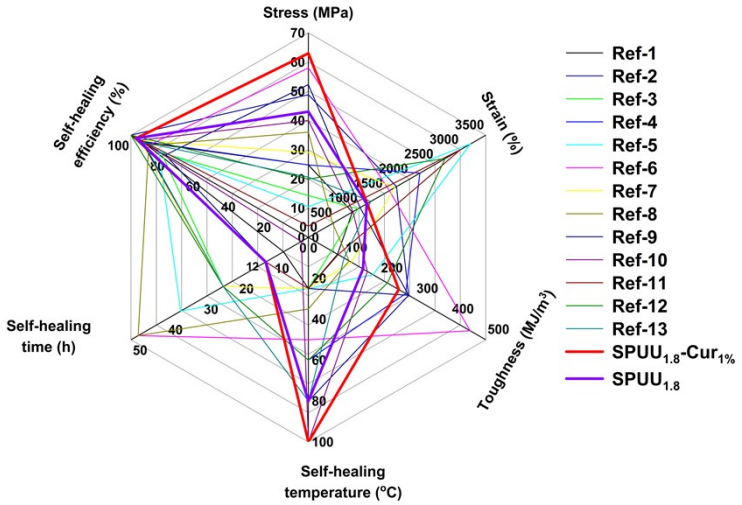

Figure S15. Comparison of mechanical properties and self-healing efficiencies between $SPUU_{1.8}$, $SPUU_{1.8}$-$Cur_{1\%}$, and recently reported self-healing polyurethane elastomers. [1-13]

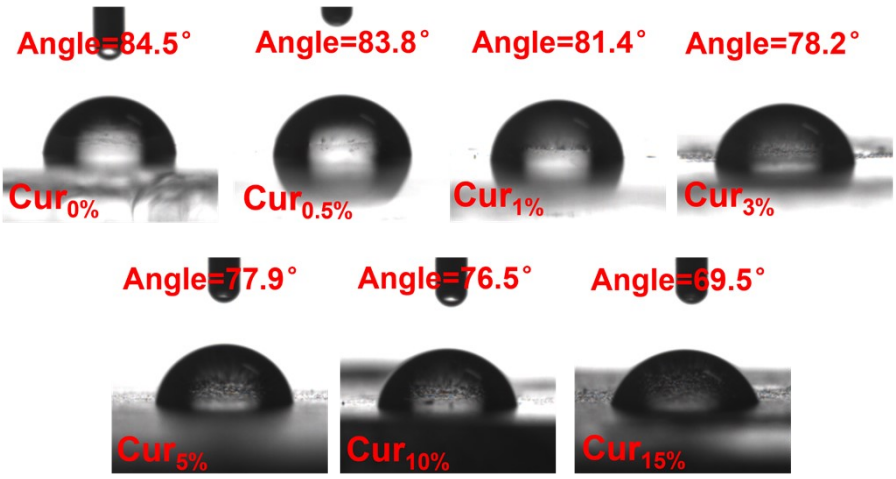

Figure S16. Contact angles of $SPUU_{1.8}$-Cur_y composites.

References

[1] X. Xun, X. Zhao, Q. Li, B. Zhao, T. Ouyang, Z. Zhang, Z. Kang, Q. Liao, Y. Zhang, Tough and Degradable Self-Healing Elastomer from Synergistic Soft-Hard Segments Design for Biomechano-Robust Artificial Skin, ACS Nano, 15 (2021) 20656-20665.

[2] X. Gao, W. Fan, W. Zhu, G. Jiuwei, P. Zhang, C. Wang, X. Wang, H. Xia, Z. Wang, W. Huang, Tough and Healable Elastomers via Dynamic Integrated Moiety Comprising Covalent and Noncovalent Interactions, Chem. Mater., 34 (2022) 2981-2988.

[3] W. Fan, Y. Jin, L. Shi, R. Zhou, W. Du, Developing Visible-Light-Induced Dynamic Aromatic Schiff Base Bonds for Room-Temperature Self-Healable and Reprocessable Waterborne Polyurethanes with High Mechanical Properties, J. Mater. Chem. A, 8 (2020) 6757-6767.

[4] F. Dong, X. Yang, L. Guo, Y. Wang, H. Shaghaleh, Z. Huang, X. Xu, S. Wang, H. Liu, Self-Healing Polyurethane with High Strength and Toughness Based on a Dynamic Chemical Strategy, J. Mater. Chem. A, 10 (2022) 10139-10149.

[5] K. Song, W. Ye, X. Gao, H. Fang, Y. Zhang, Q. Zhang, X. Li, S. Yang, H. Wei, Y. Ding, Synergy Between Dynamic Covalent Boronic Ester and Boron-Nitrogen Coordination: Strategy for Self-Healing Polyurethane Elastomers at Room Temperature with Unprecedented Mechanical Properties, Mater. Horiz., 8 (2021) 216-223.

[6] Y. Yao, B. Liu, Z. Xu, J. Yang, W. Liu, An Unparalleled H-Bonding and Ion-Bonding Crosslinked Waterborne Polyurethane with Super Toughness and Unprecedented Fracture Energy, Mater. Horiz., 8 (2021) 2742-2749.

[7] Y. Li, W. Li, A. Sun, M. Jing, X. Liu, L. Wei, K. Wu, Q. Fu, A Self-Reinforcing and Self-Healing Elastomer with High Strength, Unprecedented Toughness and Room-Temperature Reparability, Mater. Horiz., 8 (2021) 267-275.

[8] Y. Eom, S. M. Kim, M. Lee, H. Jeon, J. Park, E.S. Lee, S.Y. Hwang, J. Park, D.X. Oh, Mechano-Responsive Hydrogen-Bonding Array of Thermoplastic Polyurethane Elastomer Captures both Strength and Self-Healing, Nat. Commun., 12 (2021) 621.

[9] Y. Wang, X. Huang, X. Zhang, Ultrarobust, Tough and Highly Stretchable Self-

Healing Materials Based on Cartilage-Inspired Noncovalent Assembly Nanostructure, Nat. Commun., 12 (2021) 1291.

[10] J. Hu, R. Mo, X. Sheng, X. Zhang, A Self-Healing Polyurethane Elastomer with Excellent Mechanical Properties Based on Phase-Locked Dynamic Imine Bonds, Polym. Chem., 11 (2020) 2585-2594.

[11] T. Jing, X. Heng, X. Guifeng, C. Ling, L. Pingyun, G. Xiaode, Highly Stretchable, High Efficiency Room Temperature Self-Healing Polyurethane Adhesive Based on Hydrogen Bonds-Applicable to Solid Rocket Propellants, Polym. Chem., 12 (2021) 4532-4545.

[12] C. Xing, H. Wu, R. Du, Q. Zhang, X. Jia, Extremely Tough and Healable Elastomer Realized via Reducing the Crystallinity of Its Rigid Domain, Polym. Chem., 12 (2021) 4778-4784.

[13] C.-J. Fan, Z.-C. Huang, B. Li, W.-X. Xiao, E. Zheng, K.-K. Yang, Y.-Z. Wang, A robust self-healing polyurethane elastomer: From H-Bonds and Stacking Interactions to Well-Defined Microphase Morphology, Sci. China Mater., 62 (2019) 1188-1198.